Approximate Jacobi matrix in 3D Airborne Transient Electromagnetic inversion

Hao Ren, Da Lei
College of Earth and Planetary Sciences, University of Chinese Academy of Sciences, renhao201@mails.ucas.ac.cn
CAS Engineering Laboratory for Deep Resources Equipment and Technology, Institute of Geology and Geophysics, Chinese Academy of Sciences, leida@mail.iggcas.ac.cn

SUMMARY

In geophysical inverse problems, the computation of the Jacobi matrix is a time-consuming process that significantly limits the computational speed of the inversion. To expedite the 3D inversion process, we propose an approximation of the Jacobi matrix to speed up the computation. We utilized the approximate gradient derived from the approximate Jacobi matrix for inversion computation during each iteration, and simultaneously used an accurate forward modeling method when evaluating the quality of inversion model, so that an inversion model that satisfies the data fitting criteria could be obtained after many iterations. This approximate Jacobi matrix inversion method is applied to the 3D Airborne Transient Electromagnetic inversion of synthetic data, resulting in a significant reduction in the time required for inversion while maintaining accuracy. This technique is notably faster than traditional inversion methods that calculate the Jacobi matrix exactly, particularly when dealing with numerous model grids.

Keywords: Jacobi matrix, three-dimensional inversion, parallel computation

INTRODUCTION

The three-dimensional electromagnetic inversion of geophysics is a nonlinear, underdetermined inverse problem. Some researchers have proposed various optimization methods to address this issue, including the Gauss-Newton method(Wilson et al., 2006), quasi-Newton method(Liu and Nocedal, 1989) and conjugate gradient method(Rodi and Mackie, 2001), etc. The conjugate gradient and quasi-Newton methods only necessitate the gradient information of the objective function rather than the explicit Jacobi matrix, which means fewer adjoint forward calculations required in each inversion iteration. Despite the Gauss-Newton method requires a substantial number of forward calculations, it has markedly superior convergence speed in comparison to alternative methods. For 3D inversion of ATEM data, the time required to calculate objective function gradient explicitly is nearly equivalent to that needed to calculate the Jacobi matrix, by explicitly calculating the Jacobi matrix and constructing the Gauss-Newton inversion equation, the full advantage of the Gauss-Newton method in terms of inversion speed can be fully exploited(Yin et al., 2020).

For three-dimensional inversion problems, various methods exist for calculating the Jacobi matrix, including the perturbation method and the adjoint forward method(Liu and Yin, 2016; Zhang et al., 2021), etc. However, due to the large computational load associated with the perturbation method, researchers have increasingly turned to the adjoint forward method which processes the forward equations to derive an expression for the Jacobi matrix, followed by numerous forward calculations to obtain the Jacobi matrix.

This study proposed an approximation method for the Jacobi matrix, which can significantly reduce the number of equations that need to be solved in the adjoint forward method, thereby speeding up the computation without sacrificing inversion quality. The frequency-domain Maxwell's equations are discretized using finite difference (FD), and the equation systems are solved using Pardiso, thus, time-domain electromagnetic data is derived through a Fourier transform. The Gauss-Newton method was used to formulate the iterative formula for inversion, and the approximate Jacobi matrix was calculated to participate in the iterative computation. The stability of the method is validated by inversion results from noisy data. The results indicated that the approximate Jacobi matrix can effectively alleviate computational load and expedite the inversion process.

METHODS

3D Modeling of ATEM with IP effect

Starting from the frequency domain Maxwell equations, the following electric field equation is derived:

$$\nabla \times \nabla \times \boldsymbol{E}_s + i\omega\mu_0\sigma\boldsymbol{E}_s = -i\omega\mu_0\left(\sigma - \sigma_0\right)\boldsymbol{E}_p \qquad (1)$$

where i is the imaginary unit, ω is the angular frequency, μ_0 is the vacuum magnetic permeability, $\boldsymbol{E}_p$ is the background field, $\boldsymbol{E}_s$ is the anomalous field, and σ_0 and σ is the background and anomalous conductivity, respectively. The finite difference method is employed to discretize and solve the system of equations, thereby obtaining the frequency domain electric field. The time domain magnetic field is derived from Faraday's law and Fourier transformation, subsequently convolved with the emission waveform to ascertain the airborne aeronautical electromagnetic response for any given emission waveform(Yin et al., 2013).

The finite difference method is employed to discretize and solve the system of equations, thereby obtaining the frequency domain electric field. The time domain magnetic field is derived from Faraday's law and Fourier transformation, subsequently convolved with the emission waveform to ascertain the airborne aeronautical electromagnetic response for any given emission waveform.

The IP properties of rocks and ores are described using the Cole–Cole model(Pelton et al., 1978), which is represented by the following formula:

$$\rho\left(i\omega\right)=\rho_0\left(1-m\left(1-\frac{1}{1+\left(i\omega\tau\right)^c}\right)\right) \tag{2}$$

where ρ_0 is zero-frequency resistivity, m denotes polarizability, τ defines the time constant, and c is the frequency correlation coefficient. To generate the ATEM response that incorporates the IP properties of the rocks and ores, substitute the complex resistivity of the above equation for the real resistivity found in the forward equation.

Inversion Method

The parameters of model were updated using regularized inversion theory, where the objective function is defined as the sum of data fitting φ_{data} and model constraints φ_{model}:

$$\Phi\left(m\right)=\varphi_{data}+\lambda\varphi_{model} \tag{3}$$

Based on the Gauss-Newton method, the following iterative formula for model parameters is derived from the Equation 3:

$$\Delta\boldsymbol{m}=\left(\boldsymbol{J}^T\boldsymbol{C_d}\boldsymbol{J}+\lambda\boldsymbol{C_m}\right)^{-1}\left(\boldsymbol{J}^T\boldsymbol{C_d}\left(\boldsymbol{F}\left(\boldsymbol{m_0}\right)-\boldsymbol{d_{obs}}\right)\right) \tag{4}$$

where $\boldsymbol{m}$ is model parameters, $\boldsymbol{d_{obs}}$ is observation data, $\boldsymbol{F}\left(\boldsymbol{m_0}\right)$ is forward operator, $\boldsymbol{C_d}$ is the data weighting matrix that could balance the effect of different time-channel data on the inversion results, $\boldsymbol{C_m}$ is the model constraint matrix, which can be used to constrain the inversion results according to specific requirements, $\boldsymbol{J}$ is the Jacobi matrix, λ is the regularization factor.

Approximate Jacobi Matrix

The system of equations obtained by discretizing Equation 1 is denoted as $\boldsymbol{K}\boldsymbol{E}_s=\boldsymbol{P}$. Both sides of the equation are differentiated with respect to the model variables, and the expression for the Jacobi matrix can be obtained through the adjoint forward method(Ren et al., 2018):

$$\boldsymbol{J}^T=\left(\frac{\partial\boldsymbol{P}}{\partial\boldsymbol{m}}-\frac{\partial\boldsymbol{K}}{\partial\boldsymbol{m}}\boldsymbol{E}_s\right)^T\boldsymbol{K}^{-T}\boldsymbol{L}^T \tag{5}$$

where $\boldsymbol{P}$ is the source term, $\boldsymbol{K}$ is the forward operator, $\boldsymbol{E}_s$ is the anomalous field, and $\boldsymbol{L}$ is the interpolation operator, which is used to transfer the electric field components $\boldsymbol{E}$ to vertical magnetic field components $\boldsymbol{H}_z$. The term $\boldsymbol{v}=\boldsymbol{K}^{-T}\boldsymbol{L}^T$, derived from the solution of $\boldsymbol{K}\boldsymbol{v}=\boldsymbol{L}^T$, is substituted into equation 5 to obtain the frequency domain Jacobi matrix. Finally, the Jacobi matrix in the time domain is obtained by Fourier transform.

In practical computations, the model is integrated into N_m grids and N_p measurement points. To accurately derive the Jacobi matrix, the interpolation operator $\boldsymbol{L}$ must be of size $\left(N_m,3\times N_m\right)$. This necessitates the calculation of Nm sets of equations to ascertain the partial derivatives at the $\boldsymbol{H}_z$ component recording points. However, there often exists a discrepancy between actual measurement points and the positions of the $\boldsymbol{H}_z$ components. Consequently, an additional interpolation is required to obtain the partial derivatives at the actual measurement points. This approach demands the computation of a total of $N_p\times N_m$ sets of forward equations, which is significantly large. We propose constructing an interpolation operator of size $\left(n,3\times N_m\right)$ near each measurement point (where n represents the number of $\boldsymbol{H}_z$ recording points within the measurement point vicinity), thereby replacing global interpolation with local interpolation. As a result, only $n\times N_p$ sets of equations need to be computed to obtain the partial derivative values in the vicinity of the measurement points. Furthermore, we eliminate the second interpolation and directly employ the average partial derivatives at the $\boldsymbol{H}_z$ recording points in the measurement point vicinity as the partial derivatives at the measurement points. In 3D simulations, N_p is significantly less than N_m , thereby substantially reducing the number of equations required for computation.

Results

To validate the efficacy of the approximate Jacobi matrix method, we developed a theoretical model for an inversion test(Lei et al., 2024). The transmitting coil has a radius of 15 meters and a sending current of 100 A. Both the transmitting and receiving coils are positioned 30 meters above ground level, with a total of 121 measurement points. In the model depicted in Figure 1, the space is segmented into a grid of $28\times28\times18$. The oblique low-resistivity polarized body is embedded in a uniform half-space, with the surrounding rock resistivity at 200 Ω·m, a polarization rate of 0.01, a time constant of 0.0001, and a frequency correlation coefficient of 0.01. The target body resistivity is 50 Ω·m, with a polarization rate of 0.5, a time constant of 0.005, and a frequency correlation coefficient of 0.5. Initial model for inversion was a uniform half-space with a resistivity of 100 Ω·m, a polarization rate of 0.1, a time constant of 0.001, and a frequency correlation coefficient of 0.1.

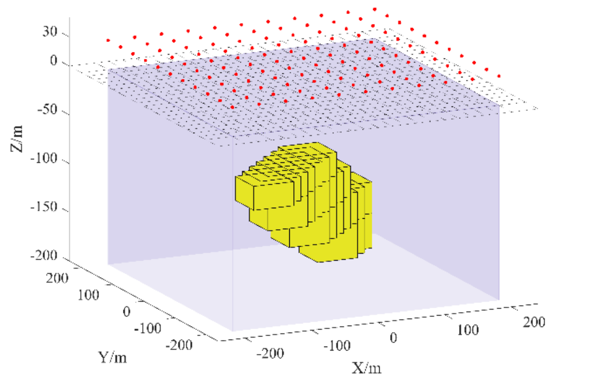

Figure 1. Schematic diagram of the model. The red points are the locations of the sampling points, and the internal oblique body is the low-resistivity polarized body.

We calculated the ATEM response of this model, and added random noise of various degrees as observational data. Using the approximate Jacobi matrix method for 3D inversion, we achieved satisfactory results. Here, we only presented the XOY horizontal slice at $z=-130m$ (Figure 2). The inversion outcomes of the four IP parameters can aptly represent the position of the actual target body. Furthermore, the results from the noisy data suggested that the approximate Jacobi matrix does not compromise the stability of the inversion algorithm.

The impact of different levels of approximation of the Jacobi matrix on the computational speed was investigated. Specifically, we replaced the values of the Jacobi matrix at the measurement point location with the averages of 1, 2, 3, and 4 H_z recording points within the measurement point neighborhood. The iteration time corresponding to approximate Jacobi matrix were compared with that of the precise Jacobi matrix. Figure 3 presents that the approximate method can provide approximately a threefold speedup in our grid, and the more meshes the model has, the more significant the acceleration effect.

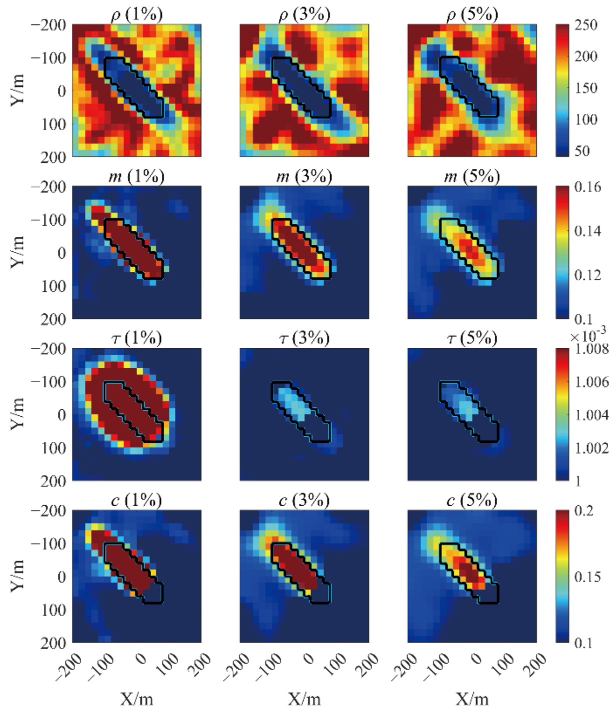

Figure 2 The XOY slice at z = −130 m shows the inversion results for four IP parameters with various noise levels.

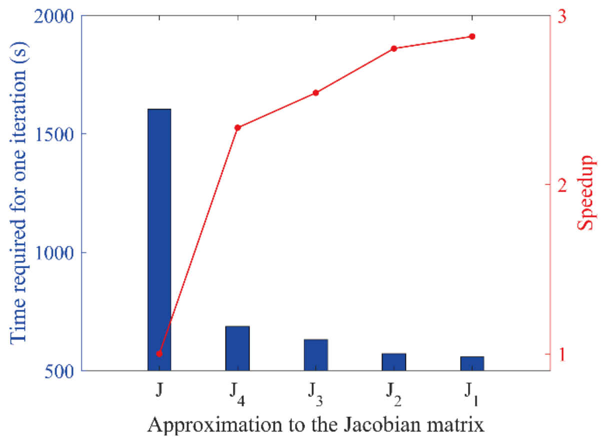

Figure 3 The effect of various approximation degrees of Jacobian matrix on calculation speed.

Conclusions

We propose an approximate Jacobi matrix method to expedite the 3D inversion of ATEM data. The approach significantly diminishes the number of systems of equation need to calculate, yielding a speedup of threefold or more during large-scale inversion. Inversion outcomes from noisy data suggest that this method is effective in determining the location and morphological characteristics of subterranean target bodies, thereby establishing it as a robust inversion technique. The approximate Jacobi matrix method presented herein can be broadened to inversion of various geophysical methods, thereby reducing computational demands and fostering the advancement of large-scale 3D inversion.

ACKNOWLEDGEMENTS

The paper is financially supported by the National Natural Science Foundation of China (42374170), the Beijing Science and Technology Plan “Deep Earth Exploration Technology Breakthrough” special project of China (Z181100005718001).

REFERENCES

Lei, D., H. Ren, R. Wang, Z. Wang, and C. Fu (2024) Parallel Inversion of 3D Airborne Transient Electromagnetic Data Using an Approximate Jacobi Matrix. Remote Sensing 16: 11.

Liu, D. C., and J. Nocedal (1989) On the limited memory BFGS method for large scale optimization. Mathematical Programming 45: 503-528.

Liu, Y., and C. Yin (2016) 3D inversion for multipulse airborne transient electromagnetic data. Geophysics 81: E401-E408.

Pelton, W. H., S. H. Ward, P. G. Hallof, W. R. Sill, and P. H. Nelson (1978) Mineral Discrimination and Removal of Inductive Coupling with Multifrequency IP. Geophysics 43: 588-609.

Ren, X., C. Yin, J. Macnae, Y. Liu, and B. Zhang (2018) 3D time-domain airborne electromagnetic inversion based on secondary field finite-volume method. Geophysics 83: E219-E228.

Rodi, W., and R. L. Mackie (2001) Nonlinear conjugate gradients algorithm for 2-D magnetotelluric inversion. Geophysics 66: 174-187.

Wilson, G. A., A. P. Raiche, and F. Sugeng (2006) 2.5D inversion of airborne electromagnetic data. Exploration Geophysics 37: 363-371.

Yin, C., W. Huang, and F. Ben (2013) The full-time electromagnetic modeling for time-domain airborne electromagnetic systems: Chinese Journal of Geophysics (in Chinese) 09: 3153-3162.

Yin, C., Y. Liu, and B. Xiong (2020) Status and prospect of 3D inversions in EM geophysics. Science China Earth Sciences 63: 452-455.

Zhang, B., C. Yin, Y. Liu, X. Ren, V. C. Baranwal, and B. Xiong (2021) 3D inversion of large-scale frequency-domain airborne electromagnetic data using unstructured local mesh. Geophysics 86: E333-E34.